RSC Advances

ROYAL SOCIETY OF CHEMISTRY

www.rsc.org/advances

www.rsc.org/xxxxxx

COMMUNICATION

Preparation and antibacterial activity of copper nanoparticles/halloysite nanotubes nanocomposites via reverse atom transfer radical polymerization

Xiaoxu Ding [a], Huixian Wang [b], Weihang Chen [a], Jindun Liu [a], and Yatao Zhang*[a]

Copper nanoparticles supported halloysite nanotubes with a 15 nm lumen and 30 nm external diameter via surface initiation reverse atom transfer radical polymerization was fabricated and showed good antibacterial activity against *Escherichia coli* (*E. coli*).

Copper nanoparticles (Cu NPs) have been considered as a promising antibacterial materials due to their high surface-to-volume-ratio, and antimicrobial activity against a wide range of microorganisms including bacteria, fungi, algae and viruses. [1-3] Several methods have been employed for the preparation of Cu NPs, including chemical reduction methods [4-6], radiation techniques [7], thermal decomposition [8], and so on. Among the above mentioned methods, chemical reduction, such as $NaBH_4$ solution, is usually used to the production of Cu NPs because of its simple process. Recently, Cu NPs with excellent stability were prepared based on polymeric micelles after the addition of reducing agent such as $NaBH_4$ [4]. However, Cu NPs are easily aggregated to result in the decrease of antibacterial property. Therefore, it is desirable to use an inorganic material as a support for loading of Cu NPs, which could reduce the aggregation of the nanoparticles.

Halloysite nanotubes (HNTs) are a type of aluminosilicate clay which possess predominantly hollow tubular structure in the submicron range, large specific surface area and is chemically similar to kaolin.[9-11] Therefore, HNTs is more suitable to act as the support of antibacterial nanoparticles. Very importantly, compared with other similar minerals, such as carbon nanotubes (CNTs), HNTs are readily obtainable, far less expensive and more easily modified. To our knowledge, up to now, only silver nanoparticles supported on HNTs were studied and reported.[12-14]

In order to make HNTs have the capability of loading copper ions, 4-vinylpyridine was chosen to modify HNTs, which has the ability of complexing transition metals by the pyridine ring and thus could act as a multidentate ligand.[15] Atom transfer radical polymerization (ATRP) allows for the polymerization of most vinyl monomers in a controlled/"living" manner onto the nanoparticles surface.[16] Poly (4-vinylpyridine) (P4VP) brushes of different length were grafted onto HNTs via surface-initiated atom transfer radical polymerization (SI-ATRP) by Jiang et al.[17] However, there are two major drawbacks for ATRP, the halide species RX are toxic and not easily handled or obtained, and the catalysts Mt^n/L_X are easily oxidized.[18-20] To overcome the drawbacks, reverse atom transfer radical polymerization (RATRP) has recently been explored. Unlike ATRP, for RATRP process, a conventional radical initiator, 2, 2'-azobisisobutyronitrile (AIBN), is used instead of the organic halide initiator RX. The metal catalyst (CuCl) was replaced by more stable catalyst ($CuCl_2$).

In this study, P4VP brushes of different length were grafted onto HNTs via RATRP to provide the pyridine rings and Cu NPs was immobilized onto HNTs with two steps, including complexation and reduction. HNTs discovered by our group in He'nan province, China was used as the support for loading of Cu NPs. For the antibacterial test, *Escherichia coli* (*E. coli*) were selected. The antibacterial test showed that Cu NPs/HNTs had good antibacterial activities. The overall preparation process of Cu NPs/HNTs is illustrated in schematically in Fig. 1.

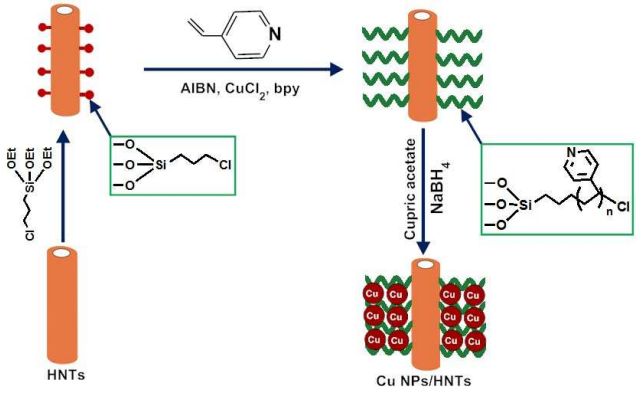

Fig. 1 Schematic illustration of the overall preparation process of Cu NPs/HNTs

Halloysite nanotubes (HNTs) with a 15 nm lumen, 30 nm external diameter, and length of 600±200 nm were developed as a support for loading of Cu NPs. HNTs was initially modified with 3-chloropropyltrimethoxysilane (CPS) in toluene (refluxing for 48 h). The resulting material was collected by centrifugation and washed several times to remove excess modifier and possible products of hydrolysis. The modified HNTs were dried overnight in an oven at 60°C under vacuum. FT-IR analysis was performed to check the grafting of CPS at the surface of HNTs and shown in Fig. 2 (a). In the spectrum of the modified HNTs, the characteristic peaks of CPS were detected at 2928 and 2858 cm^{-1}, which are attributed to asymmetric and symmetric CH_2-stretching vibration, these two peaks have originated from the C-H in CPS. Then, P4VP brushes of different length were grafted onto modified HNTs via RATRP. The polymerization was carried out in cyclohexanone as solvent and using 4-vinylpyrinde as the monomer. A mixture of predetermined amount of the reaction components were stirred and degassed via three freeze-pump-thaw cycles. The reaction flask was sealed and placed in a 75°C oil bath for a predetermined period of time. The products were

centrifuged and washed with acetone and then dried overnight in an oven at 60°C under vacuum. Fig. 2 (a) shows FTIR spectra of the modified HNTs with P4VP. It can be seen that the absorption peaks at 1601 and 1556 cm^{-1} are attributed to the pyridine ring C=N stretching vibration, the peak at 1416 cm^{-1} attributed to pyridine ring C=C stretching vibration. This proves that the P4VP was successfully grafted from HNTs by RATRP. To further confirm that the grafting polymerization is controlled, P4VP brushes were obtained by dissolution of HNTs in the HF/HCl mixture acid. The molecular weight of P4VP, as determined with GPC, increased with the polymerization time (Fig. 2 (b)). It is also seen that the molecular weight distribution of P4VP keep at around 1.40. These results confirm that P4VP brushes had been grafted onto HNTs by a living polymerization.

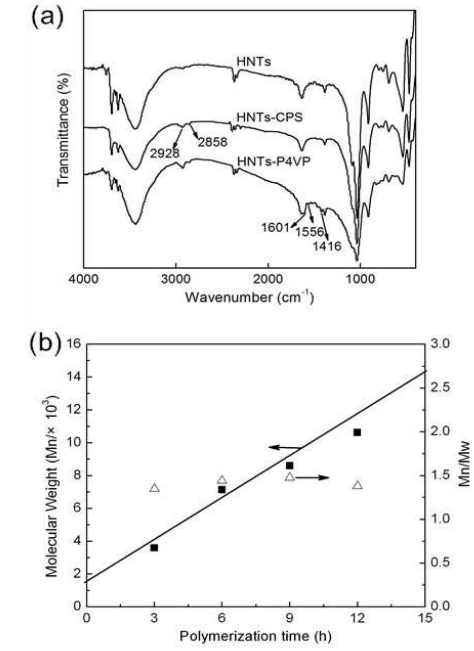

Fig. 2 FTIR spectra of HNTs, HNTs-CPS and HNTs-P4VP (a) and Evolution of Mn and Mw/Mn vs polymerization time (b)

The modified HNTs with P4VP were immersed in copper acetate solution in a shaker for 24 h at 60°C. A complex between pyridine rings of P4VP brushes and copper ions formed, leading to large clusters on the surface of HNTs. Then, these copper clusters were converted into copper nanoparticles (Cu NPs) with about 10 nm diameter by $NaBH_4$ reduction (1 mM $NaBH_{4(aq)}$ for 24 h at 100°C under the protection of nitrogen) which were homogeneously distributed and bound to the surface of HNTs. The resulting material was separated by centrifugation (6000 rpm) for 30 min, washed several times with DI water and then passivated with a mixture of oleic acid and acetone (the volume ratio is 1:10). Finally, the products were collected by centrifugation and washed with ethanol and dried overnight in an oven at 50°C under vacuum. Fig. 3 displays transmission electron microscopy (TEM) images of HNTs (a), modified HNTs with P4VP (b) and HNTs loaded with Cu NPs (c). As can be seen in the TEM images (a) and (b), the surface of modified HNTs with P4VP becomes roughness compared with the pristine HNTs and the inner diameter decreased, some even completely filled with polymer brush. Therefore, the results also demonstrated that P4VP was successfully grafted onto the surface of HNTs. Fig. 3 (c) clearly shows that Cu NPs appeared uniformly distributed across the surface of HNTs and the average diameter is about 10 nm. In addition, a homogeneous component distribution as concluded from the energy-dispersive X-ray analysis (EDX) element maps were obtained by STEM-EDX and shown in Fig. 4. Four typical elements including O, Al, Si and Cu were observed and attributed to HNTs and Cu NPs. Therefore, judging from the above results, the Cu NPs supported halloysite nanotubes (Cu NPs/HNTs) was fabricated successfully.

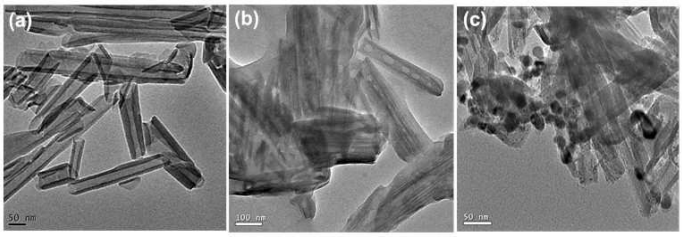

Fig. 3 TEM images of HNTs (a) modified HNTs with P4VP (b) and HNTs loaded with Cu NPs (c)

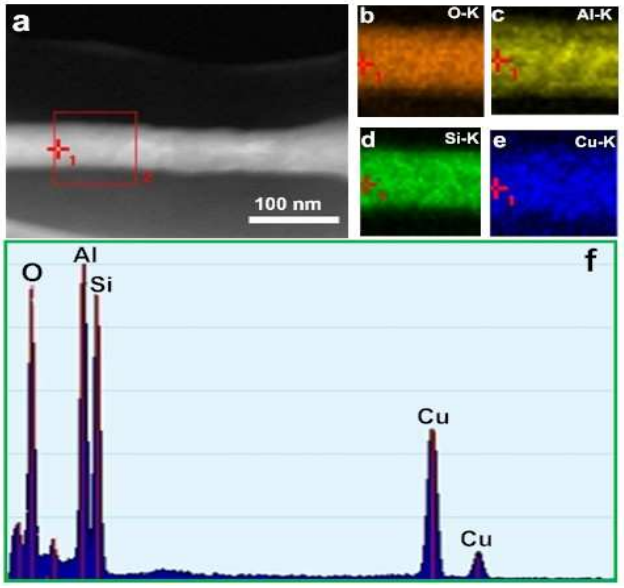

Fig. 4 Element mapping of Cu NPs/HNTs via EDX: image (a) is the sample; images (b, c, d, and e) exhibit the element sensitive maps of oxygen, aluminum, silicon, and copper. The complete element distribution is seen in the EDX spectrum in (f)

To evaluate the antibacterial properties of Cu NPs/HNTs, *E. coli* (8099) provided by College of Public Health of Zhengzhou University was selected as Gram-negative bacteria. One method of measuring the effectiveness of an antibacterial agent is to determine its minimal inhibitory concentrations (MIC) using the tube double dilution method. Serial dilutions of the antibacterial

material were performed in Mueller-Hinton broth which were inoculated with 5×10^5 CFU/mL of bacteria and incubated overnight at 37°C for 8 h. Growth of the cells was determined by observing the turbidity of the culture. The lowest concentration of Cu NPs/HNTs, at which no visual turbidity could be observed, represented the MIC of the antibacterial material. Generally, the turbidity of suspension increased with the decrease of the antibacterial material concentration, and the MIC of Cu NPs/HNTs against *E. coli* were observed to be 128 $\mu g \cdot mL^{-1}$. Moreover, the number of remaining bacteria was examined to further determine the degree of the antibacterial effect in the presence of the antibacterial material. The cultures that lacked turbidity and have the lowest concentration of the antibacterial material above MIC test were reinoculated into fresh LB media to test their ability to grow. 100 μL of the above suspension after being diluted 10^5 times was cultured on an agar plate then incubated at 37°C for 16 h and the numbers of colonies were counted. As shown in Fig. 5, the bacteria colonies on the culture plates are observed as small white dots. It can be seen that fewer colonies were formed on the nutrient agar plates after the exposure to the Cu NPs/HNTs. The antibacterial rate of the Cu NPs/HNTs against *E. coli* was as high as 90.7% and indicates that Cu NPs/HNTs possessed good antibacterial activity. This effective antibacterial performance of Cu NPs/HNTs could be explained by the large surface areas of the nano-size particles (Cu NPs). Copper nanoparticles could lead to increase in number of particles per unit area and, thus, antibacterial effects could be maximized. The unique structure of HNTs supporting highly dispersed Cu clusters could lead to superior antibacterial properties. In such a configuration, Cu clusters are largely fixated on HNTs surfaces, which improve their aggregation in aqueous suspensions. This configuration could enhance Cu/bacteria contact and antibacterial efficiency in attacking and destructing bacterial cell membranes.

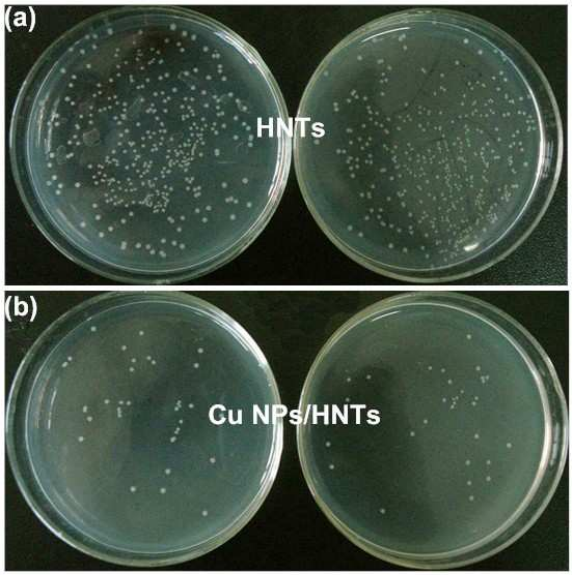

Fig. 5 Photographs showing the bacterial culture plates of *E. coli* upon a 16 h exposure to HNTs (a) and Cu NPs/HNTs, 128 $\mu g \cdot mL^{-1}$ (b)

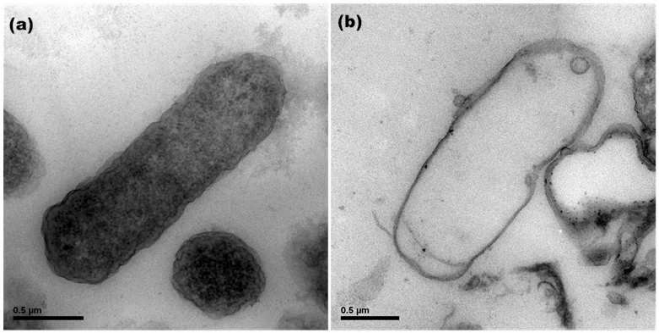

Fig. 6 TEM images of *E. coli* cells treated with HNTs (a) and Cu NPs/HNTs (b)

The antibacterial mechanism of copper is not yet fully understood. At least one mechanism has been proposed to interpret the antibacterial activities of copper. That is, Cu nanoparticles could attach to the bacterial cell membrane, causing structural changes or functional damages and inhibit their growth, up to the cell's death. In this study, the supported Cu NPs, which are compactly loaded on HNTs surfaces, could have highly centralized interactions with the cell membrane upon contact. Increased damage to the membrane could be expected from the crowded Cu clusters. Herein, TEM images were performed to observe the morphology changes of *E. coli* cells treated with HNTs and Cu NPs/HNTs. *E. coli* cells treated with Cu NPs/HNTs solution for 30 min were fixed with 2.5% glutaraldehyde. The cells were washed with PBS and then postfixed with 1% aqueous OsO4 (Fluka) for 1 h and washed again twice with PBS. The cells then were dehydrated through ethanol series (70% for 15 min, 90% for 15 min, and 100% for 15 min twice) and embedded in Epon/Araldite resin (polymerization at 65°C for 15 h). Thin sections (90 nm) containing the cells were placed on the grids and stained for 1 min each with 4% uranyl acetate (151 acetone/water) and 0.2% Raynolds lead citrate (water), air dried, and examined under a transmission electron microscope (FEI, USA). The TEM results are shown in Fig. 6. The images revealed that *E. coli* cells treated with Cu NPs/HNTs lost cellular integrity, with the cell membrane being destroyed and the cytoplasm flowing out, which lead to the death of *E. coli* cells.

Recently, another more important mechanism of action have been proposed that the dissipation of cell membrane potential from the formation of cell filaments and formation of reactive oxygen species (ROS), can damage the bacterial cell membrane and bacterial DNA, which can cause protein oxidation and result in bacterial cell death. [21]

In conclusion, a novel antibacterial agent, Cu NPs with 10 nm diameter supported halloysite nanotubes (Cu NPs/HNTs) was firstly fabricated successfully, which showed good antibacterial activity against *E. coli*. It is anticipated that copper nanoparticles supported halloysite nanotubes could be used in various applications in the bioadhesive, antibacterial fabrics, and antibacterial membrane.

Acknowledgements

This work was supported by National Natural Science Foundation of China (Nos. 21106137, 21376225 and 21276244) and China Postdoctoral Science Foundation (Nos. 2014T70686 and 2013M531684).

Notes and references

[a] *School of Chemical Engineering and Energy, Zhengzhou University, No. 100 of Science Road, Zhengzhou 450001, China. Fax: +86-371-67781734; Tel: +86-371-67739348; E-mail: zhangyatao@zzu.edu.cn*
[b] *School of Civil Engineering and Communication, North China University of Water Resources and Electric Power, Zhengzhou 450045, China*

(1) B. Biswajoy, D. Sumit, B. Suman, D. Sukhen, B. Alakananda, B. Ruma and N. Papiya, *Mater. Sci. Eng., C*, 2012, **32**, 1897.
(2) Y. H. Kim, D. K. Lee, H. G. Cha, C. W. Kim, Y. C. Kang and Y. S. Kang, *J. Phys. Chem. B*, 2006, **110**, 24923.
(3) D. Longano, N. Ditaranto, N. Cioffi, F. Di Niso, T. Sibillano, A. Ancona, A. Conte, M. A. Del Nobile, L. Sabbatini and L. Torsi, *Anal. Bioanal. Chem.*, 2012, **403**, 1179.
(4) H. Lu, L. Lu, B. Yang, J. Si and J. Du, *Rsc Adv.* 2014, **4**, 14193.
(5) K. Zhang, *Appl. Surf. Sci.,* 2012, **258**, 7327.
(6) A. K. Chatterjee, R. K. Sarkar, Veerabadran, A. P. Chattopadhyay, P. Aich, R. Chakraborty and T. Basu, *Nanotechnology,* 2012, **23**, 085103.
(7) Y. Teng, J. Zhou, F. Luo, G. Lin and J. Qiu, *J. Non-Cryst. Solids,* 2011, **357**, 2380.
(8) Y. H. Kim, D. K. Lee , B. G. Jo, J. H. Jeong and Y. S. Kang, *Colloids Surf., A*, 2006, **284-285**, 364.
(9) Y. Chen, Y. Zhang, J. Liu, H. Zhang and K. Wang, *Chem. Eng. J.,* 2012, **210**, 298.
(10) Y. Chen, Y. Zhang, H. Zhang, J. Liu, and C. Song, *Chem. Eng. J.,* 2013, **228**, 12.
(11) Y. M. Lvov, D. G. Shchukin, H. Möhwald and R. R. Price, *ACS nano,* 2008, **2**, 814.
(12) Y. Zhang, Y. Chen, H. Zhang, B. Zhang and J. Liu, *J. Inorg. Biochem.*, 2013, **118**, 59.
(13) L. Yu, Y. Zhang, B. Zhang, and J. Liu, *Sci. Rep.*, 2014, **4**, 4551.
(14) P. Liu, M. Zhao. *Appl. Surf. Sci.*, 2009, **255**, 3989.
(15) J. Qiu, Y. Zhang, Y. Zhang, H. Zhang and J. Liu. *J. Colloid Interf. Sci.,* 2011, **354**, 152.
(16) C. Wan, M. Li, X. Bai, and Y. Zhang, *J. Phys. Chem. C,* 2009, **113**, 16238.
(17) J. Jiang, Y. Zhang, D. Cao and P. Jiang, *Chem. Eng. J.,* 2013, **215-216**, 222.
(18) Y. Chen, Q. Deng, J. Xiao, H. Nie, L. Wu, W. Zhou and B. Huang, *Polymer,* 2007, **48**, 7604.
(19) D. Qin, S. Qin and K. Qiu, *J. Appl. Polym. Sci.,* 2001, **81**, 2237.
(20) S. Jin, N. Zhou, D. Xu, Y. Wu, Y. Tang, C. Lu, J. Zhang and J. Shen, *Colloids Surf., B,* 2013, **101**, 319.
(21) A. K. Chatterjee, R. Chakraborty, and T. Basu, *Nanotechnology*, 2014, **25**, 135101.

